Intramolecular Hydrogen Bonding in Disubstituted Ethanes. A Comparison of NH···O$^-$ and OH···O$^-$ Hydrogen Bonding through Conformational Analysis of 4-Amino-4-oxobutanoate (succinamate) and Monohydrogen 1,4-Butanoate (monohydrogen succinate) Anions

Mark S. Rudner, Senka Jeremic, Krag A. Petterson, David R. Kent, IV, Katherine A. Brown, Michael D. Drake, William A. Goddard, III, and John D. Roberts*

Gates and Crellin Laboratories of Chemistry and Materials and Process Simulation Center of the Beckman Institute, California Institute of Technology, Pasadena, California 91125

Received: June 1, 2005

Relative strengths of amide NH···O$^-$ and carboxyl OH···O$^-$ hydrogen bonds were investigated via conformational analysis of succinamate and monohydrogen succinate anions with the aid of vicinal proton−proton NMR couplings and B3LYP DFT quantum mechanical calculations for a variety of solvents. New experimental results for succinamate are compared with those obtained from previous studies of monohydrogen succinate. While some computational results for monohydrogen succinate were published previously, the results contained herein are the product of a more powerful methodology than that used earlier. The experimental results clearly show that intramolecular hydrogen-bond formation is more favored in aprotic solvents than in protic solvents for both molecules. Furthermore, the preference of the succinate monoanion for the gauche conformation is much stronger in aprotic solvents than that of succinamate, indicating that the OH···O$^-$ hydrogen bond is substantially stronger than its NH···O$^-$ counterpart, despite the ∼5 kcal cost for formation of the E configuration of the carboxyl group needed to make an intramolecular hydrogen bond. The actual energy differences between formation of internal hydrogen bonds for monohydrogen succinate and succinamate anion were estimated by comparison of the relative values of K_1 of the respective acids in water and DMSO by a procedure first developed by Westheimer. Recent theoretical work with succinamate highlights the necessity of considering substituent orientational degrees of freedom to understand the conformational equilibria of the central CH_2-CH_2 torsions in disubstituted ethanes. Similar methodology is applied here to succinic acid monoanion, by mapping potential-energy surfaces with respect to the CH_2-CH_2 torsional, carboxyl-substituent rotational, and carboxyl−proton E/Z isomeric degrees of freedom. Boltzmann populations were compared with gauche populations estimated from the experimentally determined coupling constants. The quantum mechanical results for succinamate show a much weaker tendency toward hydrogen bonding than for the succinic acid monoanion. However, the theoretical methods employed appear to substantially overestimate contributions from intramolecularly hydrogen-bonded structures for the succinic acid monoanion when compared with experimental results. Natural bond orbital analysis, applied to the quantum mechanical wave functions of fully optimized gauche and trans structures, showed a strong correlation between the population of amide σ^*_{N-H} and carboxyl σ^*_{O-H} antibonding orbitals and apparent hydrogen-bonding behavior.

Introduction

Hydrogen bonding from amide hydrogens and carboxyl protons to negative oxygen is a feature of some biological motifs.[1−3] Because such bonding can occur in a large number of environments, for example, potentially in all peptides containing ionized aspartate residues, we have investigated its influence on the conformational preferences of 4-amino-4-oxobutanoate (succinamate, **1**) and monohydrogen 1,4-butanoate (monohydrogen succinate, **2**) in a variety of solvents. The conformational equilibrium is expected to be affected by the formation of the corresponding intramolecularly hydrogen-bonded gauche-type structures, **1a** and **2a**.

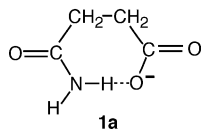

1a

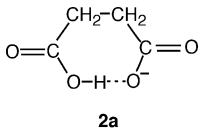

2a

In previous work,[4] we reported on the lack of evidence for intramolecular hydrogen bonding for **2** in water, which would involve **2a**. Although this finding was unexpected by many, it is supported by the trends seen in the conformational equilibria of **2** in a variety of solvents,[5] as well as by stochastic Monte Carlo classical explicit-solvent simulations.[6] Why is **2a** so unimportant in water? We can cite several contributing factors: one is the 4−5 kcal/mol penalty associated with converting the more stable Z configuration of the carboxyl proton to the E configuration needed to form an intramolecular hydrogen bond.[6] Another factor is water's apparent efficiency in solvating the relatively open trans structure with its exposed polar carboxyl and anionic carboxylate groups.[6,7] There is also a possible unfavorable entropy change arising from cyclization. Additionally, the geometrical constraints on intramolecular hydrogen-bond formation may not be optimal for maximum strength.

When we compare the hydrogen-bonded ratios of **1a** with **2a**, we expect the ratio [**1a**]/[**1**] to be smaller than [**2a**]/[**2**] on

10.1021/jp052925c CCC: $30.25
Published on Web 09/17/2005

the basis that an amido N−H bond is less polar than a carboxyl O−H bond. In **1a**'s favor, however, is the fact that the aforementioned penalty associated with converting the carboxyl OH from Z to E required by **2a** is not required for the amide.[6] Some information is available from quantum calculations and the infrared spectrum of succinamic acid and related compounds,[8−10] but we have no record of NMR determinations of conformational equilibria of succinamic acid and **1**, possibly because these entities do not appear superficially to offer much conformational interest.

Experimental Procedures

Our studies to determine the proportion of **1** existing as **1a**, as well as the conformational preferences of succinamic acid itself, utilized the NMR and analytical techniques for the estimations of conformational equilibria described earlier.[4,5,11] Solutions in nonaqueous solvents were prepared by dissolution of succinic acid (Aldrich) or of succinamic acid with 1 equiv or more of 95% tetrabutylammonium cyanide (Aldrich)[12] in the appropriate deuterated solvent using a drybox.[7] If there was uncertainty as to whether the salt-forming reaction was complete, the cyanide and acid were dissolved in methanol and taken to dryness under reduced pressure. In other research, we have found this procedure to be effective with acids that are much stronger than HCN in water, but relatively weaker in solvents such as dimethyl sulfoxide (DMSO).[7,13,14]

Quantum Mechanical Calculations

All quantum-mechanical calculations reported here were made with Jaguar version 4.2 release 77 (Schrodinger, Inc.) using Becke 3-LYP type density functional theory.[15] In our initial work with succinamate monoanion, we found it necessary to use large, triple-ζ basis sets with diffuse functions to approach convergence of results. Thus, we report here results for succinamate monoanion and succinic acid monoanion as calculated with the 6-311G**++ and (aug)-cc-pVTZ(-f) basis sets.[16−19]

Solution-phase calculations were modeled using the continuum-solvation approximation. The parameters and limitations of this method as used in our calculations are discussed elsewhere.[20]

Generation of Potential-Energy Surfaces

Because of its relevance to observed NMR proton−proton couplings and its role in determining the qualitative geometric features of molecular conformations of 1,2-disubstituted ethanes, the CH_2-CH_2 bond dihedral angle plays a central role in both experimental and theoretical work on disubstituted ethanes of the sort studied herein. For some systems, other degrees of freedom, such as the motion of the substituent groups, can influence the equilibrium of the CH_2-CH_2 torsional degree of freedom. In other recent work with **1**,[20] we found that accounting for the rotational motion of the amide substituent as an additional statistical degree of freedom had a significant effect on the results. Thus, we concluded that such degrees of freedom should not generally be ignored in calculations of conformational equilibria.

In addition to the CH_2-CH_2 torsional and carboxyl group rotational degrees of freedom, **2** has a third degree of freedom that we can expect to play a significant role in its conformational equilibria. There are two possible configurations for the hydroxyl of the carboxyl group, labeled E and Z, respectively (see Figure 1). Hydrogen bonding to the opposing carboxylate group is only possible from the less stable E-form. Because the expected energy of interconversion from Z to E is the same order of magnitude as the expected enthalpy of hydrogen-bond formation, one would expect the CH_2-CH_2 torsional equilibrium to depend on a delicate balance of energetic and entropic contributions from all three of the cited degrees of freedom.

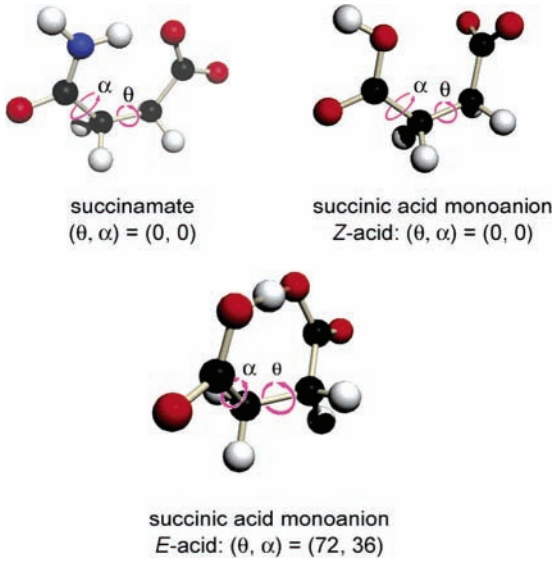

Figure 1. The angle θ is defined as the central CCCC dihedral of particular interest, while α defines the orientation of one of the substituents.

Two-dimensional potential-energy surfaces (PESs) were generated for each system with coordinates corresponding to the CH_2-CH_2 and substituent (amide or carboxyl) torsional degrees of freedom.[20] Because of limited computational resources, the out-of-plane rotational degree of freedom of the carboxyl OH of **2** could not be treated in detail. A two-state model for this degree of freedom was adopted; two separate two-dimensional PESs were generated, *one each* for the carboxyl E- and Z-isomers. Boltzmann population analysis was then carried out on the set of states consisting of the union of all states on the E-carboxyl and Z-carboxyl two-dimensional surfaces.

Figure 1 shows the angles that we have varied in our calculations. As a shorthand for referring to specific conformers, we label them by the values of these two angles using the notation (θ, α). In generating the PESs, (θ, α) were confined to 36° increments in both directions on the domain [0°, 360°] × [0°, 360°] (see Figure 2). For **2**, the un-ionized carboxyl OH rotation was allowed to relax adiabatically to the most stable E-like and Z-like positions. Altogether, 121 calculations were performed for each **1** system, and 242 calculations were performed for each **2** system. Although symmetry arguments could be used to reduce the number of required calculations significantly, we performed all of the redundant calculations using nonequivalent starting structures to minimize the risk of getting caught in local minima during geometry optimizations. The required symmetries of the PESs were then enforced after the fact, by assigning the minimum energy of any set of symmetrically equivalent points to all such points.

For plotting and statistical analysis, the PESs were fit in θ and α with a two-dimensional cubic spline surface and interpolated onto a finer grid with a spacing of 9° in both directions. A Boltzmann distribution was assumed for the discrete states on the fine grid and the relative popu-

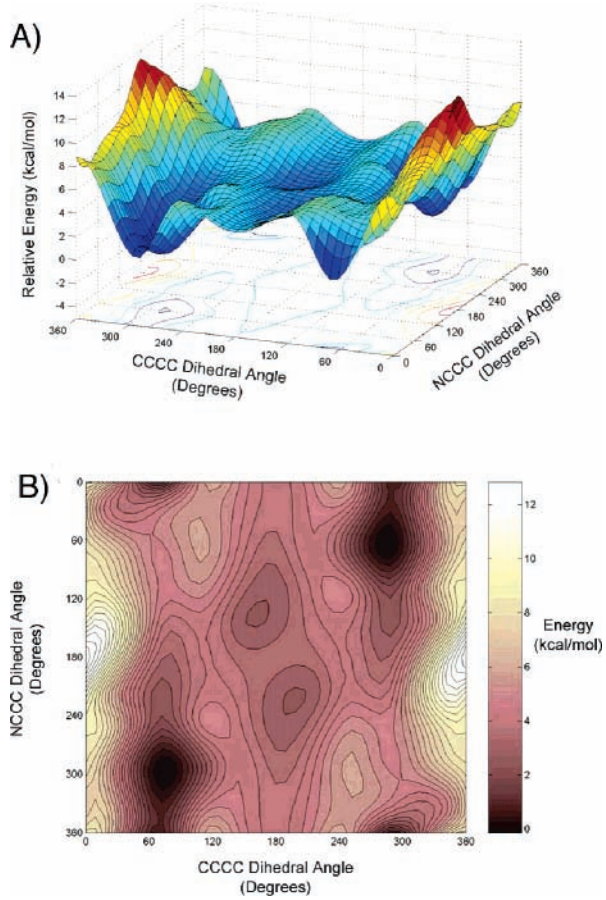

Figure 2. An example of a 2D potential-energy surface as calculated in this study. (A) The PES is for succinamate in acetone. (B) A shaded contour map of the PES for succinamate in acetone.

lations calculated by

$$f^{\lambda}_{(\theta,\alpha)} = \frac{\exp(-\Delta E^{\lambda}_{(\theta,\alpha)}/kT)}{\sum_{\theta,\alpha,\lambda} \exp(-\Delta E^{\lambda}_{(\theta,\alpha)}/kT)} \quad (1)$$

where $f^{\lambda}_{(\theta,\alpha)}$ is the relative amount of the species with dihedral angles θ and α as defined earlier and $\lambda \in \{E, Z\}$ indicating the E/Z isomerism for **2**, $\Delta E^{\lambda}_{(\theta,\alpha)}$ is the energy of the (4-carboxyl) conformer (θ, α), k is the Boltzmann constant, and T is the absolute temperature. The θ-rotamer populations were calculated by summing the probabilities over α (and, of course, the E and Z configurations) for each value of θ

$$f_{\theta} = \sum_{\alpha,\lambda} f^{\lambda}_{(\theta,\alpha)} \quad (2)$$

For comparison, we also calculated the populations considering only the lowest-energy structure for each value of θ

$$f^{ad}_{\theta} = \frac{\exp(-E^{\min}_{\theta}/kT)}{\sum_{\theta} \exp(-E^{\min}_{\theta}/kT)} \quad (3)$$

with

$$E^{\min}_{\theta} = \min_{\alpha,\lambda} E^{\lambda}_{(\theta,\alpha)} \quad (4)$$

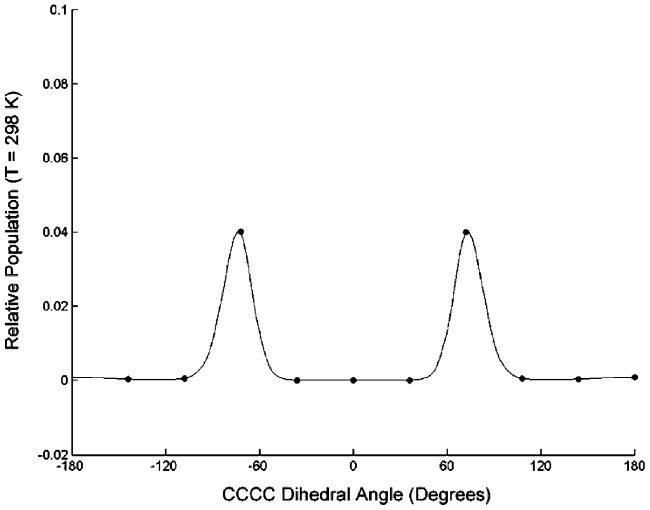

Figure 3. After summation over the α-coordinate, a 1D probability distribution for θ is produced. The measured J_{13} and J_{14} coupling constants are, in principle, statistically averaged over all conformations of the CCCC dihedral according to this distribution.

This procedure thus recreated the results of the simpler one-dimensional adiabatic model (see Figure 3).

Further analyses of structures of types **1** and **2** were carried out by performing full geometry optimizations to obtain optimized gauche and trans structures for each case. Natural bond orbital (NBO) analysis[19] was then applied to the resulting wave functions to look for evidence of hydrogen bonding. Diagonalization of monoatomic and diatomic sub-blocks of the 1-particle density matrix results in the creation of 1-center lone pair/core orbitals and 2-center bonding orbitals of high occupancy, along with their Rydberg/antibonding counterparts of low occupancy.[21] Examination of the occupancies of these orbitals can lead to useful insight about the bonding within and between molecules as will be shown below.

Results and Discussion

Experimentally determined J_{13} and J_{14} coupling constants, gauche populations estimated from these values, and amide proton chemical shifts for succinamic acid and its monoanion are presented in Table 1. The corresponding values for succinic acid monoanion are presented in Table 2. For succinamic acid itself, **3** represents the most likely mode of intramolecular hydrogen bonding, because the acidic proton is much less tightly bound than the amide protons, and for the carboxyl group to be able to hydrogen bond efficiently to the NH_2 group, the latter would have to be distorted out of normal amide group planarity. It does not appear, however, that **3** has a significant influence on the conformational preferences of succinamic acid, as little or no preference for the gauche conformation is observed in alcohols and aprotic solvents, where one would expect intramolecular hydrogen bonding to be most favored, if at all. Indeed, in seven alcohols and aprotic solvents ranging from methanol to tetrahydrofuran (THF), the conformational mix was within ±4% of the statistical 2:1 ratio.

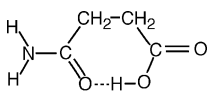

3

The situation with **1** is different. When compared in terms of acidity, an amide N−H proton is much more tightly bound

TABLE 1: Experimental Vicinal $^1H-^1H$ Couplings, Chemical Shifts, and Estimated Gauche Conformational Preferences for Succinamic Acid and Its Monoanion in Various Solvents

	succinamic acid							succinamate						
solvent	expt J_{13} Hz	expt J_{14} Hz	% G^a (J_{13})	% G^a (J_{14})	% G^a avg	δ_{N-H} ppm	$\delta_{N-H'}$ ppm	expt J_{13} Hz	expt J_{14} Hz	% G^a (J_{13})	% G^a (J_{14})	% G^a avg	δ_{N-H} ppm	$\delta_{N-H'}$ ppm
D_2O	7.61	5.97	77 67	78 68	78 68	n/a	n/a	6.85	8.28	59 51	57 50	58 51	n/a	n/a
methanol	6.97	6.97	64 56	68 59	66 58	n/a	n/a	6.47	9.26	51 45	48 42	50 44	n/a	n/a
ethanol	7.20	7.20	68 60	66 57	67 59	n/a	n/a	6.89	8.48	59 52	55 48	57 50	n/a	n/a
tert-butyl alcohol	7.03	7.76	65 57	61 53	63 65	n/a	n/a	7.92	5.86	80 69	80 69	80 69	n/a	n/a
acetone	7.57	6.15	76 66	76 67	76 67	6.959	6.299	9.04	3.90	102 89	98 85	100 87	n/a	n/a
DMSO[b]	7.04	6.93	65 57	68 60	67 59	7.303	6.774	8.41	5.32	89 78	85 74	87 76	8.424	6.246
dioxane[c]	6.95	6.95	63 55	68 60	66 58	6.286	6.019	8.67	4.46	94 82	93 81	94 82	8.242	5.824
THF	7.22	7.22	69 60	66 57	67 59	6.610	6.130	9.13	3.08	103 90	105 92	104 91	9.819	5.519

[a] Altona procedure[12−14]-calculated gauche populations for $\theta_g = 60°$ (left) and $\theta_g = 70°$ (right). [b] The succinamic acid sample contained 0.5× as many moles of water as the succinamate anion in DMSO. [c] The succinamic acid sample contained 30× more moles of water than the succinamate anion in dioxane.

TABLE 2: Previously Determined Conformational Preferences of Monohydrogen Succinate

solvent	% G ($\theta_g{}^a = 60°$)	% G ($\theta_g{}^a = 70°$)
D_2O[b]	66	57
methanol[b]	78	68
ethyl alcohol[b]	87	76
tert-butyl alcohol[b]	>100	99
DMSO[c]	>100	100
THF[d]	>100	100

[a] θ_g is the angle used as the gauche angle between the 1,2-substituents in the Altona procedure for the calculation of % G. [b] Ref 20. [c] Ref 9. [d] Ref 5.

than a carboxyl hydroxyl proton [pK_a(amide) − pK_a(−CO_2H) ≈ 12], $\Delta\Delta G \approx 17$ kcal/mol. Consequently, an important factor expected to bear on the ease of formation of **1** relative to **2** is the acidities of the carboxyl groups of the corresponding acids, when the statistical factor of 2 favoring succinic acid is taken into account. While succinic acid is stronger than succinamic acid in water, where the pK_a's are 4.19 and 4.54, respectively,[22] it is actually very close to the statistical ratio. Of course, the situation could be more complex in solvents other than water because of differences in the ability of the medium to solvate anionic species. A basis for evaluating this effect was provided by Westheimer and Benfey[23] for dibasic acids through the comparison of K_1 of a given acid and that of its monomethyl ester (K_E). If $K_1 > 2K_E$, then one can infer some degree of stabilization of the monoanion relative to the monoester anion, most likely by intramolecular hydrogen bonding as exemplified by **2a**.

This technique was exploited by McCoy[24] to determine optimal hydrogen-bonding geometries and by Kolthoff[25] in studies of K_1/K_2, which for succinic acid in water is about 25, but is about 10^7 in DMSO.[25,26] This, along with the fact that $K_1/K_E = \sim 10^3$ for succinic acid, shows that there is important hydrogen-bond stabilization of **2** in DMSO as solvent. That this is the result of formation of **2a** is confirmed by, as far as we can tell from the coupling constants, exclusive formation of a gauche conformer.[7] This is in contrast to the situation in aqueous solution in which the gauche and trans forms coexist quite close to the 2:1 statistical equilibrium ratio.[4] Another data point is provided by K_1/K for succinic and succinamic acids. In water, as already mentioned, the difference is essentially the statistical factor of 2. In DMSO, we used the method described earlier[26] to show the pK_a of succinamic acid to be 11.78. Comparing this with pK_1 = 9.5 for succinic acid, we find the ratio of the same ionization constants to be 95 (again taking into account the statistical factor of 2). If we neglect entropy effects, this gives an estimated 3.1 kcal/mol greater strength of the hydrogen bond of **2a** compared to **1a** in DMSO, which comes to 8 kcal/mol after the additional ∼5 kcal/mol correction is made for the conversion of the Z to the E isomer to allow intramolecular hydrogen-bond formation to occur.

The relevance of all this to the formation of **1a** is that, in water, **1** shows some preference for the trans conformer (58:42 gauche/trans) and even more so in methanol (50:50). However, the trend reverses for ethanol and *tert*-butyl alcohol, in which the ratios are 57:43 and 80:20, respectively. If we assume that the increase in importance of the gauche conformer relative to its importance in methanol results from the formation of **1a**, we need to correct the coupling constants predicted for ethanol and *tert*-butyl alcohol for the certainty that the dihedral angle of **1a** is larger than 60°, probably closer to 70°.

How do we know this? In DMSO[27] and THF,[7] we have a strong argument that **2** is, for practical purposes, all gauche. Its NMR spectrum, assuming staggered dihedral angles, corresponds to 110% gauche, but to 100% with gauche dihedral angles of 70°. This correction reduces the preferences for **1a** in ethanol and *tert*-butyl alcohol to 50:50 and 69:31, respectively. Nonetheless, the trend mirrors the behavior of **2** in the same alcohols,[5] although the extent of preference for the gauche conformer is much smaller with the N−H···O$^-$ system than for an intramolecular O−H···O$^-$ hydrogen bond, even with the latter having an E to Z conversion expense of 5 kcal/mol.

In addition to the DMSO argument, the supposition of a gauche minimum at an angle greater than 60° for **2a** is strongly supported by our quantum-mechanical calculations (see Tables 3 and 4 for a summary of our quantum-mechanical results for **1** and **2,** respectively). The center of the gauche well, as defined by the first moment of the Boltzmann probability distribution (eq 5) over the gauche states with CCCC dihedral between 0° and 120°, is consistently near 65° across all solvents for succinate monoanion and near 75° for succinamate**.** We have interpreted our succinamate experimental results in terms of gauche angles of 60° and 70°.

$$\theta_G = \frac{\sum_{\theta=0°}^{\theta=120°} \theta f_\theta}{\sum_{\theta=0°}^{\theta=120°} f_\theta} \qquad (5)$$

In aprotic solvents, **1a** again appeared to be less favorable than **2a**. The trend for **1**, based on a 75° dihedral angle, was DMSO (76:24), dioxane (82:18), acetone (88:12), and THF (91:9). For comparison, **2** is 100% **2a** in both DMSO and THF. The importance of **1a** in these aprotic solvents is confirmed by

TABLE 3: Summary of ab Initio Results for Succinamate Anion

basis set	θ^a (dioxane)	% G (dioxane)	% $G_{ad}{}^b$ (dioxane)	θ (acetone)	% G (acetone)	% $G_{ad}{}^b$ (acetone)	θ (water)	% G (water)	% $G_{ad}{}^b$ (water)
6-311G**++	75°	100%	100%	77°	60%	82%	74°	66%	90%
aug-cc-pVTZ(-f)	75°	100%	100%	76°	62%	82%	77°	42%	55%

[a] θ is the average gauche angle from the mean of the population distribution over all gauche conformers. [b] % G_{ad} values were calculated from the adiabatic one-dimensional energy curves.

TABLE 4: Summary of Ab Initio Results for Succinate Monoanion

basis set	θ^a (dioxane)	% G (dioxane)	% $G_{ad}{}^b$ (dioxane)	θ (acetone)	% G (acetone)	% $G_{ad}{}^b$ (acetone)	θ (water)	% G (water)	% $G_{ad}{}^b$ (water)
6-311G**++	65°	100%	100%	65°	100%	100%	65°	100%	100%
aug-cc-pVTZ(-f)	65°	100%	100%	65°	100%	100%	65°	100%	100%

[a] θ is the average gauche angle from the mean of the population distribution over all gauche conformers. [b] % G_{ad} values were calculated from the adiabatic one-dimensional energy curves.

the difference in chemical shifts between the E and Z protons of the amide nitrogen that can be ascribed in a straightforward way to hydrogen bonding. With succinamic acid itself, this difference in parts per million was DMSO, 0.53; dioxane, 0.27; acetone, 0.66; and THF, 0.48. With the monoanion, the chemical shifts paralleled the calculated fractions of gauche and were DMSO, 2.18; dioxane, 2.42; and THF, 4.30.

The predictions of the conformational equilibria of **1** from our quantum mechanical simulations are shown in Table 3. Table 4 shows the results for **2**. A clear trend is visible in the succinamate results with the aug-cc-pVTZ(-f) basis set, indicating that the gauche population in dioxane should be greater than the gauche population in acetone, which should also be significantly greater than the gauche population in water. We trust these results the most, because they were obtained with the largest and presumably best basis set available. While the experimental results also indicate a low gauche population in aqueous solution, the observed gauche population was *greater* in acetone than in dioxane. However, this could be the result of some degree of complexation of **1a** with the acetone carbonyl carbon as shown by **4**.

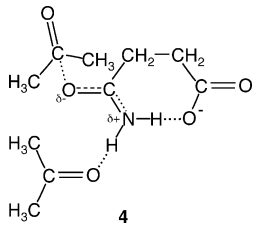

4

Such complexation could increase the acidity of the *E*-NH proton. Analogous effects involving acetone as solvent have been observed in other conformational equilibria[28] but are not included in the solvent-continuum model used in this study. Recent improvements in the software's solvation model may handle these effects more appropriately and lead to improved results.

The situation for **2** looks less promising. The simulations predicted gauche populations of 100% in all three solvents in contrast to the experimental observations which showed nearly statistical proportions in water, and only a moderate preference for gauche in dioxane.

As discussed elsewhere,[20] the inclusion of substituent rotational effects led to a significant change in the predictions for the conformational equilibria of **1**. A similar effect was not observed in our simulations of **2** because of the overwhelming effect of the hydrogen-bonded states. On the basis of the **1** results, however, we still recommend exploring as many potentially influential degrees of freedom as possible in any conformational study of this sort.

TABLE 5: Natural Bond Orbital Analysis of the E and Z Forms of Succinate Monoanion and Succinamate Ion

Succinate Monoanion				
	gauche		trans	
(O_1-H_9 σ^* NBO occupation)	E-acid	Z-acid	E-acid	Z-acid
		Acetone		
cc-pVTZ(-f)++	0.1827	0.01044	0.00629	0.01067
6-311G**++	0.17961	0.01023	0.00633	0.01036
		H_2O		
cc-pVTZ(-f)++	0.18127	0.01054	0.0062	0.01019
6-311G**++	0.17792	0.01031	0.00622	0.00987
		Dioxane		
cc-pVTZ(-f)++	0.20119	0.01117	0.00669	0.01132
6-311G**++	0.19804	0.01097	0.00672	0.01113
Succinamate Ion				
	gauche		trans	
($N-H$ σ^* NBO occupation)	N_1-H_{10}	N_1-H_9	N_1-H_{10}	N_1-H_9
		Acetone		
cc-pVTZ(-f)++	0.03146	0.0118	0.00738	0.01002
		H_2O		
cc-pVTZ(-f)++	0.02874	0.01215	0.00772	0.00956
		Dioxane		
cc-pVTZ(-f)++	0.05481	0.01355	0.00846	0.01098

In agreement with the experimental observations, the simulations show that **2a** is significantly more favorable than **1a.** Examination of the natural bond orbitals produced in the NBO analysis reveals a strong correlation between occupancy of the σ^*_{O-H} and σ^*_{N-H} antibonding orbitals and apparent hydrogen-bonding behavior. To investigate this correlation, fully optimized gauche and trans structures were found for **1** and **2** (both E and Z isomers) in each of the three solvents. Although the absolute occupations of the natural bond orbitals calculated with 6-311G**++ and aug-cc-pVTZ(-f) differed slightly as expected, the trends between the different conformers and molecular species appeared to be in complete agreement. The results of the NBO analysis with the aug-cc-pVTZ(-f) basis set are presented in Table 5. For **1**, H_9 is the amide hydrogen directed away from the carboxylate, and H_{10} is the amide hydrogen directed toward the carboxylate.

The most important features of the **1** data are as follows: (a) In gauche conformations, the σ^*_{N-H} orbital has a significantly larger occupation for the bond directed towards the carboxylate than the σ^*_{N-H} orbital on the opposite side (**5a**), and (b) there appears to be a "base" occupation of around 0.01 that is

observed for both N−H bonds in trans conformations and in the non-hydrogen-bonded pair in gauche conformations. This control/variable analysis shows a strong correlation between σ^*_{N-H} orbital occupation and the hydrogen-bonding interaction. Furthermore, the trend in the conformational preference for the gauche conformation is mirrored in the occupations of σ^*_{N-H10} across the three solvents.

For **1**, the E/Z isomerism offers another opportunity for a control/variable test of the correlation between hydrogen-bonding behavior and σ^*_{O-H} orbital occupation. Similar to what was observed for **2**, there seems to be a base occupation of approximately 0.01 for σ^*_{O-H} in non-hydrogen-bonded configurations. Contrary to the case for **1**, where the hydrogen-bonded σ^*_{N-H} orbitals had occupations of only a few percent, the significantly stronger OH···O$^-$ hydrogen bonds lead to σ^*_{O-H} occupations of nearly 20% (**5b**). This is also mirrored by the significantly stronger preference toward gauche exhibited in the **2** conformational equilibrium predictions.

Although the simulations did not yield predictions of the conformational equilibria in close agreement with experimental observations, the self-consistency of the equilibrium calculations and NBO analysis does suggest a useful correlation between O−H/N−H antibonding orbital occupation and hydrogen-bonding behavior. Using the occupation of these antibonding orbitals as a measure of hydrogen-bond strength, we see that the OH···O$^-$ is significantly stronger than its NH···O$^-$ counterpart.

Within the limitations of the theoretical methods used, the OH···O$^-$ mode of hydrogen bonding appears to be very insensitive to the choice of solvent. This may be related to the large degree of hydrogen bonding predicted in aqueous solvent, contradictory to the observed nearly statistical distribution. A likely culprit is the continuum-solvent model, which in the form used in this work does not account for specific interactions between solvent and solute molecules.

Conclusions

The message of all our results is clearly that an intramolecular OH···O$^-$ hydrogen bond is much stronger than its NH···O$^-$ counterpart, particularly if one takes into account the 5 kcal/mol required to convert its Z form to its E form, which is stereoelectronically capable of internal hydrogen-bond formation. Further, we find that aprotic media are needed for intramolecular hydrogen bonds for **1** and **2** to become dominant in their conformational equilibria.

Also, as has been seen in other systems such as β-alanine[11] and the dianion of succinic acid,[7] where the solute is expected to interact strongly with the solvent, the continuum-solvent model runs into difficulty in bringing out differential solvation effects between gauche and trans conformers in water. Explicit solute−solvent effects are expected to be strongest in D_2O and weakest in dioxane, which also mirrors the observed discrepancy in the difference between the experimental and theoretical results. It appears that full explicit-solvent calculations are necessary to capture such effects, especially for cases such as these where there is a competition between intramolecular and intermolecular (solute−solvent) hydrogen bonding and possibly other specific solute−solvent interactions. Improvements made to the continuum solvent model since the time of these calculations may lead to better agreement with experimental results at less cost than performing full explicit-solvent calculations.

Although substituent orientation effects were shown to be important in calculations of the conformational equilibria of succinamate, this was not the case for succinic acid monoanion because of the predicted large degree of hydrogen bonding. Nonetheless, the importance of this effect on the predicted equilibria for succinamate suggests that substituent orientation effects should be considered in future calculations.

Finally, the NBO analysis indicated a strong correlation between hydrogen-bonding behavior and OH/NH antibonding orbital occupation. This leads to a useful picture **5** of hydrogen bonding, where a hydrogen bond is formed when lone-pair electrons are able to delocalize into nearby σ^*_{X-H} orbital.

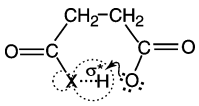

5a, X = HN; **5b**, X = O

Acknowledgment. Acknowledgment is made to the donors of the Petroleum Research Fund administered by the American Chemical Society, for support of this research. We are also deeply indebted to the National Science Foundation under grant CHE-0104273, the Summer Undergraduate Research Fellowship Program (SURF) at the California Institute of Technology, the Senior Scientist Mentor Program of the Camille and Henry Dreyfus Foundation, the E. I. Du Pont Company, and Dr. & Mrs. Chester M. McCloskey for their helpful financial assistance. D.R.K. is grateful for support of this research by a graduate fellowship from the Fannie and John Hertz Foundation. The computational resources at the MSC were provided by ARO-DURIP and ONR-DURIP. Other support for the MSC came from DOE, ONR, NSF, NIH, Chevron-Texaco, Nissan, Aventis, Berlex, Intel, and the Beckman Institute.

References and Notes

(1) Waltho, J. P.; Williams, D. H. *J. Am. Chem. Soc.* **1989**, *111*, 2475−2480.
(2) Pervushin, K.; Billeter, M.; Siegal, G.; Wuethrich, K. *J. Mol. Biol.* **1996**, *264*, 1002−1012.
(3) Reiling, K. K.; Krucinski, J.; Miercke, L. J. W.; Raymond, W. W.; Caughey, G. H.; Stroud, R. M. *Biochemistry* **2003**, *42*, 2616−2624.
(4) Lit, E. S.; Mallon, F. K.; Tsai, H. Y.; Roberts, J. D. *J. Am. Chem. Soc.* **1993**, *115*, 9563−9567.
(5) Williams, L. N.; Petterson, K. A.; Roberts, J. D. *J. Phys. Chem. A* **2002**, *106*, 7491−7593.
(6) Price, D. J.; Roberts, J. D.; Jorgenson, W. L. *J. Am. Chem. Soc.* **1998**, *120*, 9672−9679.
(7) Kent, D. R., IV; Petterson, K. A.; Gregoire, F.; Snyder-Frey, E.; Hanely, L. J.; Muller, R. P.; Goddard, W. A.; Roberts, J. D. *J. Am. Chem. Soc.* **2002**, *124*, 4481−4486.
(8) Antonenko, N. S. *Zh. Obshch. Khim.* **1965**, *85*, 425−429.
(9) Gregory, M. J.; Loadman, M. J. R. *J. Chem. Soc. B* **1971**, 1862−1865.
(10) Aleman, C.; Navarro, E.; Puiggali, J. *J. Org. Chem.* **1995**, *60*, 6135−6140.
(11) Gregoire, F.; Wei, S. H.; Streed, E. W.; Brameld, K. A.; Fort, D.; Hanely, L. J.; Walls, J. D.; Goddard, W. A.; Roberts, J. D. *J. Am. Chem. Soc.* **1998**, *120*, 7337−7343.
(12) The commercial samples we have used of 95% tetrabutylammonium cyanide give a strong ^{19}F NMR signal at the tetrafluoroborate chemical shift. This impurity is unlikely to affect our results, although on some occasions, it may have accounted for slightly soluble residues.
(13) Bordwell, F. G. *Acc. Chem. Res.* **1988**, *21*, 456−463.
(14) Nair, G.; Roberts, J. D. *Org. Lett.* **2004**, *5*, 3699−3701.
(15) Becke, A. D. *J. Chem. Phys.* **1993**, *98*, 5648−5652.
(16) Hehre, W. J.; Ditchfield, R.; Pople, J. A. *J. Chem. Phys.* **1972**, *56*, 2257−2261.
(17) Hariharan, P. C.; Pople, J. A. *Theor. Chim. Acta* **1973**, *28*, 213−222.
(18) Krishnan, R.; Binkley, J. S.; Seeger, R.; Pople, J. A. *J. Chem. Phys.* **1980**, *72*, 650−654.
(19) Foster, J. M.; Boys, S. F. *Rev. Mod. Phys.* **1960**, *32*, 300−302.
(20) Rudner, M. S.; Kent, D. R., IV; Goddard, W. A., III; Roberts, J. D. *J. Phys. Chem. A* **2005**, *109*, 9083−9088.
(21) Foster, J. P.; Weinhold, F. *J. Am. Chem. Soc.* **1980**, *102*, 7211−7218.

(22) Jeffrey, G. H.; Vogel, A. I. *J. Chem. Soc.* **1934**, 1101−1105.
(23) Westheimer, F. H.; Benfey, O. T. *J. Am. Chem. Soc.* **1956**, *78*, 5309−5311.
(24) McCoy, L. L. *J. Am. Chem. Soc.* **1967**, *89*, 1673−1677.
(25) Kolthoff, I. M.; Chantooni, J. M. K.; Bhowmik, S. *J. Am. Chem. Soc.* **1968**, *90*, 23−28.
(26) Choi, P. J.; Petterson, K. A.; Roberts, J. D. *J. Phys. Org. Chem.* **2002**, *15*, 278−286.
(27) Petterson, K. A. Unpublished experiments in dimethyl sulfoxide, 2003.
(28) Yousif, G. A.; Roberts, J. D. *J. Am. Chem. Soc.* **1988**, *90*, 6428−6431.